JACS
JOURNAL OF THE AMERICAN CHEMICAL SOCIETY

ARTICLE

pubs.acs.org/JACS

Anchor Group versus Conjugation: Toward the Gap-State Engineering of Functionalized ZnO(10$\bar{1}$0) Surface for Optoelectronic Applications

Arrigo Calzolari,*[,†,⊥] Alice Ruini,[‡,§] and Alessandra Catellani[∥]

[†]Theory@Elettra Group, Democritos Simulation Center, CNR-IOM Istituto Officina dei Materiali, I-34012 Trieste, Italy

[‡]Centro S3, CNR-Istituto di Nanoscienze, I-41125 Modena, Italy

[§]Dipartimento di Fisica, Università di Modena e Reggio Emilia, I-41125 Modena, Italy

[∥]CNR-IMEM, Parco Area delle Scienze, 37A, I-43100 Parma, Italy

Supporting Information

ABSTRACT: Molecular sensitization of the single-crystal ZnO (10$\bar{1}$0) surface through absorption of the catechol chromophore is investigated by means of density functional approaches. The resulting type II staggered interface is recovered in agreement with experiments, and its origin is traced back to the presence of molecular-related states in the gap of metal−oxide electronic structure. A systematic analysis carried out for further catecholate adsorbates allows us to identify the basic mechanisms that dictate the energy position of the gap states. The peculiar level alignment is demonstrated to be originated from the simultaneous interplay among the specific anchoring group, the backbone conjugation, and the lateral functional groups. The picture derived from our results provides efficient strategies for tuning the lineup between molecular and oxide states in hybrid interfaces with potential impact for ZnO-based optoelectronic applications.

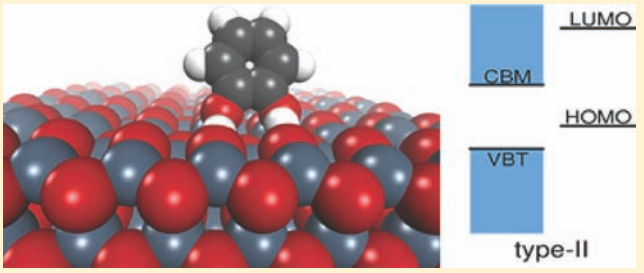

INTRODUCTION

Nanostructured semiconductors, including metal−oxides (e.g., TiO_2, ZnO, MgO), chalcogenides (e.g., CdS, CdSe, CdTe), and nitrides (e.g., GaN, InP), are foreseen as promising and efficient materials for a large set of optoelectronic devices such as light emitters, sensors, lasers, and solar cells. The specific operation of such different devices is mainly related to the peculiar electronic properties of the semiconductor in the band gap region. Hence, control of gap states is fundamental for the final application, since their presence can produce disruptive effects or be of primary importance in devices that involve light coupling for very different purposes (e.g., absorption, emission, photochemical reactions). In ZnO nanoparticles, for instance, the presence of surface states in the gap wastes the emission efficiency in UV lasers, while it can be profitably exploited for detection of water contaminants in photocatalytic sensors[1] or photocatalytic water splitting.[2]

One way to design and control the distribution of states in the gap as well as to adjust the ionization potential/electron affinity level of a semiconductor system is functionalization of its surface via adsorption of suitable ligands, such as organic molecules:[3−5] formation of hybrid interfaces may allow at the same time passivation of surface defects and generation of novel nanocomposites with different properties. For example, adsorption of molecular dyes is used to tailor the optical response of metal−oxide materials (e.g., ZnO, TiO_2), making them photoactive in the visible range and thus useful as photoanodes in dye-sensitized solar cells.[6,7] Paradigmatic is the case of the adsorption of the catechol dye (1,2-dihydroxybenzene) on ZnO surface. The unique optical and electronic properties of ZnO (e.g., wide band gap) make it a promising candidate for optoelectronic devices working in the UV range (e.g., UV lasers[8]) but not in the visible or infrared region. However, after adsorption of catechol molecule (Figure 1a) the hybridized ZnO surface exhibits an optical absorption band in the visible range (∼420 nm),[1,9,10] even though the two isolated subsystems (i.e., ZnO and the isolated molecule) absorb light only in the UV. Similar sensitization effects have been reported also in the case of catechol adsorption on TiO_2 surfaces[11,12] and nanoparticles .[13−15]

Sensitization of metal−oxide semiconductors (e.g., ZnO, TiO_2) has been usually related to establishment of molecular levels in the substrate energy gap and formation of a staggered type II interface (left side of Figure 1b). This specific band distribution would allow for absorption of light and separation of electrons and holes across the interface, fast injecting photoelectrons from dye to metal−oxide. This is a not-obvious result that has been assumed as valid but whose origin has not been yet justified. In fact, since catechol has an optical gap larger than the oxide ones, formation of a type I interface (right side of Figure 1b), which does not imply introduction of molecular

Received: November 10, 2010
Published: March 28, 2011

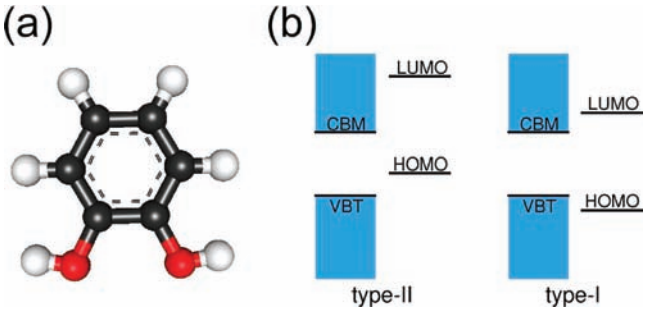

Figure 1. (a) Atomic structure of the catechol molecule. (b) Energy diagram showing the two possible band alignments occurring at the hybrid interface: type II (i.e., staggered) band offset is illustrated on the left side, while the right side shows a type I (i.e., straddling) alignment. CBM and VBT stand for the conduction band minimum and valence band top of the substrate, while HOMO (LUMO) is the highest occupied molecular orbital (lowest unoccupied molecular orbital).

states in the gap, could in principle be possible, as it happens in the case of similar small molecules (e.g., water, formic acidic) on metal−oxide surfaces (e.g., TiO_2, ZnO, MgO[16−19]) or organic molecules (e.g., benzene, styrene) on Si surfaces.[20] Formation of the two interfaces corresponds to very different optoelectronic properties that make the system suitable for different kind of applications: Straddling type I interfaces favor energy transfer, and fluorescence decays thus are used for biological tagging[21] and in light-emitting diodes,[22,23] while staggered type II interfaces favor exciton splitting and charge separation and thus are useful for devices that produce photocurrent and/or voltage drop, such as photovoltaic solar cells.[24−27] Furthermore, once a type II interface is formed, the energy position of the molecular levels inside the substrate gap, i.e., closer to the valence rather than to the conduction band, affects some characteristic properties of the final device such as the direct/inverse polarization offset of photodiodes or the open-circuit voltage in excitonic solar cells.[28] In this light, a rationale to predict lineups between molecular and semiconductor states, starting from local properties of the isolated systems, would be extremely desirable for the improvement of the final application.

In this paper, we focus on the prototypical catechol/ZnO-$(10\bar{1}0)$ interface, aiming at understanding the origin of the occurring level alignment and devising efficient strategies for its tuning. We first give an ab initio characterization of the structural and electronic properties of the catechol/ZnO interface. Then, we discuss the effects of deprotonation and water environment on the electronic structure of the interface. Finally, we investigate the optoelectronic properties of ZnO-based interfaces obtained by changing the anchor, or the external functional group, as generated from chemical modification of the prototype catechol molecule taken as the reference. In particular, we explain the origin of formation of the type II interface in terms of the electronic properties of the anchor and lateral groups. Furthermore, we propose a prescription for the control of surface states and band offset at the interface, based on the interplay between the conjugation and the electron donor/acceptor capability of the adsorbed molecule. This constitutes a step forward in the gap-state engineering of ZnO: a necessary achievement for selection of the most suited properties to be exploited in the different kinds of ZnO-based applications.

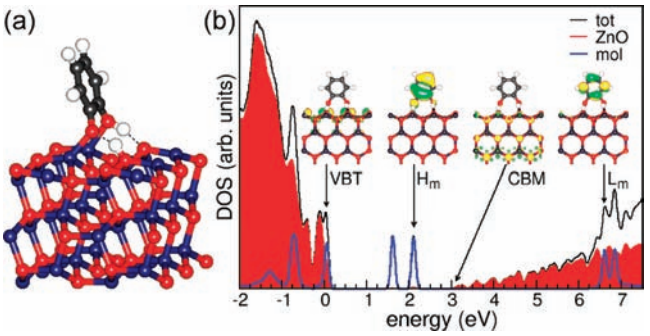

Figure 2. (a) Side view of the atomic structure of catechol adsorbed on ZnO$(10\bar{1}0)$. (b) Total DOS (black line) and projected contributions on ZnO substrate (shaded area) and catechol (blue line) for the molecule/surface interface. Inner panels show representative single-particle states.

COMPUTATIONAL DETAILS

Our results are obtained by means of plane waves, pseudopotential density functional theory (DFT) calculations, as implemented in the Quantum-ESPRESSO package.[29] We use PBE gradient correction[30] to the exchange correlation functional and ultrasoft pseudopotentials.[31] Single-particle wave functions (charge) are expanded in a plane waves basis with an energy cutoff of 28 Ry (280 Ry). The semicore 3d electrons of zinc are explicitly included in the valence shell. A 4×4 k-point grid is used for summations over the 2D Brillouin zone. The unit supercell has a 3×2 lateral periodicity and contains six bilayers of ZnO$(10\bar{1}0)$, with one catechol molecule symmetrically adsorbed on each surface. Slab replicas are separated by ∼12 Å of vacuum. Each structure is fully relaxed, until forces on all atoms become lower than 0.03 eV/Å. Detailed accuracy tests about the preparation of the starting geometries are reported in the Supporting Information.

The DFT description of ZnO bulk band structure provides a severe underestimation of the band gap (E_g^{DFT} = 0.7 eV vs E_g^{exp} = 3.3 eV), well beyond the standard gap reduction provided by DFT. In particular, the wrong energy position of the Zn 3d orbitals in the pseudopotential description causes a spurious interaction with the sp band of oxygen that is responsible for the strong underestimation of the energy gap (E_g = 0.7 eV). Since this is not strictly related to the absence of the self-energy correction, closure of the ZnO gap can be only partially improved by many-body techniques[32] unless the convergence parameters are pushed at the limits of currently computational resources, available nowadays only for the bulk system.[33]

As an alternative route, we followed a method proposed in the literature by Janotti and co-workers,[34] which includes an ad hoc Hubbard U potential, in the DFT+U scheme, to correct for the strongly underestimated band gap and improve the energy lineup of molecular states at the interface. In this framework, the Hubbard U values included in the calculations do not have to be considered as physical on-site electron−electron screened potentials, in the sense of the many-body Hubbard Hamiltonian, but as empirical parameters introduced to correct the gap.[34,35] To overcome the unphysical $Zn_{3d}-O_{2sp}$ coupling, we included a Hubbard potential U = 12.0 eV on the 3d orbitals of zinc and U = 6.5 eV on the 2p orbitals of oxygen. These specific values of U parameters result from the fit of the experimental ZnO bulk band structure:[36] the resulting Kohn−Sham gap is thus corrected to 3.1 eV.

We optimized the atomic structures at the standard DFT level (no Hubbard correction) and included the Hubbard correction only to the electronic structure (i.e., without further atomic relaxation). See section S2 of the Supporting Information for further numerical details and discussion about the effects of DFT+U correction on the structural and electronic properties of the ZnO bulk and surface.

dx.doi.org/10.1021/ja1101008 |J. Am. Chem. Soc. 2011, 133, 5893–5899

RESULTS AND DISCUSSIONS

Catechol/ZnO Interface. We first optimized the structure of the clean ZnO($10\bar{1}0$) surface that forms ordered rows of buckled Zn−O dimers along the polar [0001] direction, with a net electron accumulation on the exposed oxygen atoms. On the electronic side, surface relaxation introduces a surface state per dimer at the top of the valence band in the 2D band structure, which reduces the gap to 2.9 eV. The bottom of conduction band maintains, instead, its sp bulk-like behavior, in agreement with previous theoretical results[36] (for further details see section S2, Supporting Information). Two starting geometries were prepared by setting the catechol at ∼3.2 Å from the surface, with the phenyl ring both parallel and perpendicular to the exposed dimers. Both configurations converged to the same structure: In the final geometry (Figure 2a) the molecule has the ring oriented almost vertical and perpendicular to the [0001] direction. Catechol binds to the surface, creating two Zn−O bonds, with two consecutive surface dimers. During the relaxation path the molecule spontaneously deprotonates, releasing a H^+ ion from one hydroxyl group. The H proton is captured by the oxygen atom of the next neighbor dimer (Figure 2a). The other OH termination rotates and points toward the frontal oxygen atom of the lateral dimer. The final position of the OH groups leads to formation of two parallel H bonds with the surface. The two Zn−O bond lengths are very similar (2.1 and 2.0 Å), with the deprotonated catechol oxygen slightly closer to the Zn atom. The surface does not exhibit structural distortions, except for the adsorption sites, where the substrate derelaxes, removing only the buckling of the dimers involved in the bonding process. Formation of two covalent and two hydrogen bonds per molecule strongly stabilizes the structure. This corresponds to an adsorption energy per molecule equal to $E^{ads} = 1/2[E^{tot} - E^{surf} - 2\cdot E^{mol}] = 2.25$ eV, where E^{tot}, E^{surf}, and E^{mol} are, respectively, the total energy of the catechol/ZnO interface, the clean ZnO surface, and the pristine (fully protonated) catechol molecule. The resulting exothermic energy balance confirms that catechol is a very good linker for molecular anchorage on the ZnO($10\bar{1}0$) surface.

The density of states (DOS) of the interface is shown in Figure 2b (thin line). The shaded area and thick line identify the projection on the ZnO surface and catechol, respectively. The zero of the energy scale is fixed at the top of the valence band (VBT) of the clean surface. In low-coverage conditions, adsorption of the molecule only slightly perturbs the valence band top and the conduction band minimum (CBM) of the surface that remains similar to the clean surface case (see insets of Figure 2b and Supporting Information). Zn−O binding orbitals are detected at lower energy (ca. −1.5 eV) in the valence band and result from a charge transfer from Zn dimer atoms to catechol oxygens. This charge transfer partially restores the 4-fold coordination of surface Zn atoms, which is responsible for removal of the clean dimer relaxation, described above (see also section S3 of the Supporting Information for further details).

The gap area is dominated by the presence of two occupied molecular states, which derive from the HOMO (H_m) and HOMO−1 orbitals of the radical catechol. They are π orbitals with contributions on both the aromatic ring and the oxygen atoms. The overlap with surface states is negligible. The corresponding LUMO state (L_m) of the dye is set at higher energy (∼6.5 eV) in the conduction band. It has π character and it is partially overlapped with the ZnO electronic states at the surface.

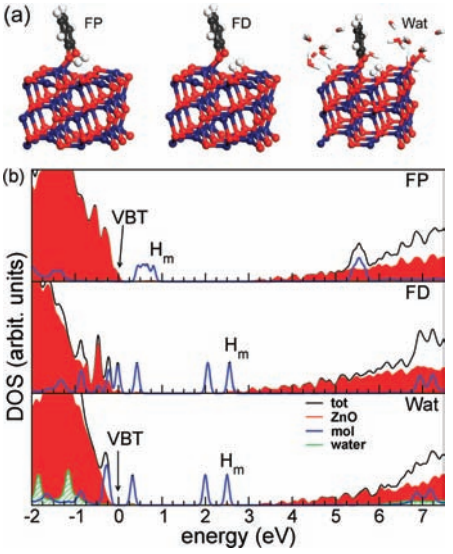

Figure 3. (a) Side view of the atomic structure of catechol adsorbed on ZnO($10\bar{1}0$) (ball and stick) in the fully protonated (FP) and fully deprotonated (FD) configurations and in the presence of water molecules (stick). (b) Total DOS (black line) and projected contributions on ZnO substrate (shaded area), catechol (blue line), and water (green area) for the molecule/surface interfaces of panel a. The zero of the energy scale is aligned to the top of the valence band of the clean ZnO surface.

The resulting effective gap of the interface (CBM-H_m) is reduced to 0.9 eV, which is consistent with an optical excitation in the visible range, i.e., adsorption of catechol translates the intrinsic optical properties of ZnO to those of a staggered type II interface, as observed in the experiments.[9,10] Incidentally, we note that because of the small number of donor (molecular HOMO) and acceptor (i.e., low DOS at bottom of conduction band of ZnO[10]) states involved in the light absorption process, catechol itself, even though a sensitizer, is not probably the best candidate for light harvesting in the visible range for photovoltaic applications. However, other lower gap catecholate molecules (e.g., anthocyanins[37,38]) may allow for a better coupling with the conduction band bottom, becoming more suitable candidates for solar cell applications.

Effects of Deprotonation. In order to gain insights into the effects of the spontaneous deprotonation accounted above, we calculated the electronic structure for the catechol/ZnO interface, forcing the molecule to be fully protonated (FP) and fully deprotonated (FD). In both cases, the adsorbed molecules maintain the same number of bonds with the surface, i.e., two Zn−O and two H bonds (Figure 3a).

The DOSs of Figure 3b are obtained keeping the atom fixed in the starting configurations, since the atomic relaxation would spontaneously restore the half-protonated geometry (i.e., the minimum energy configuration) described in the previous section. In fact, FP and FD configurations are energetically less stable than the half-protonated one by 610 and 566 meV/molecule, respectively.

Despite the fine differences in the two electronic structures, both FP and FD configurations are characterized by the presence of fully occupied molecular states in the semiconductor band gap, which is coherent with formation of a type II interface. The presence (absence) of the H^+ on the surface locally modifies the

dx.doi.org/10.1021/ja1101008 |J. Am. Chem. Soc. 2011, 133, 5893–5899

charge distribution of the surface dimer facing the molecule: this is reflected in the change of the density of states at VBT ($E \approx 0$ eV in Figure 3b). On the other side, the different number of hydrogens attached to catechol alters the charge polarization around the molecular oxygens, which affects the band alignment at the interface. We will return to this point in the next section.

The H^+ ion transfer depends on the interaction between the hydroxyl terminations of catechol and the ZnO surface dimers. This electrostatic coupling may be easily modified by the external environment such as water solution, typically present in the experimental settings.[12]

In order to simulate the effects of a polar solvent on the dye/ZnO interface, we considered (*Wat* configuration) the coadsorption of catechol and a few water molecules (eight H_2O per surface side). The starting positions of the water molecules have been taken from a representative snapshot of an ab initio molecular dynamics simulation of cyanin molecules in water, which includes catechol molecule as a lateral functional group.[39] We set a starting configuration with the hydrated molecule at ca. 3.2 Å from the surface; then we fully optimized the structure of the molecule/surface interface.

During relaxation the molecule spontaneously releases two H^+ ions from the two hydroxyl terminations. The two ions are captured by the oxygen atoms of the surface as shown in Figure 3a. Catechol binds to the surface similarly to the dehydrated case, forming two Zn−O bonds with the surface. Part of the water molecules (four of eight) bind to the surface and fully saturate the remaining surface dimers (i.e., those not involved in the bonding with catechol). Some of them spontaneously dissociate in order to optimize formation of a H-bonding path with the surface, in agreement with previous results;[16,19] others establish H bonds with the hydroxyl groups of catechol, changing the local electron polarization and promoting complete molecule deprotonation (see also Figure S7, Supporting Information). The remaining four H_2O molecules orient in space to optimize the number of H bonds with the rest of the functionalized interface. This complex adsorption/dissociation interplay maximizes the formal number of H bonds at the interface and reduces the electrostatic repulsion between H atoms, stabilizing the final geometry. Hence, in the resulting configuration, all the surface Zn atoms are involved in chemical bonds with adsorbate oxygen atoms (both from catechol and water) and all the oxygens are engaged in formation of H bonds. The number of released H^+ ions results from the interplay between steric repulsion and covalent/hydrogen bond formation with both the substrate and the adsorbate molecules (see below).

Total and projected DOSs for *Wat* interface are shown in Figure 3b. Even though water does not directly introduce further states into the ZnO gap area, it induces two specific effects: First, adsorbing on surface dimers (Zn sites) water fully saturates the ZnO surface states. In fact, by comparing DOSs with (Figure 3b) and without (Figure 2b) water, we can recognize the same spectral features (e.g., H_m, L_m, CBM), except for the VBT peak that disappeared in the *Wat* configuration (vertical arrow). In the clean surface or in a low-dosage regime (e.g., Figure 2b), the VBT peak corresponds to dimer surface states. In the present case, instead, the surface states are completely saturated by the adsorption of both catechol and water molecules. Second, water locally changes the dielectric properties of the interface, as proved, for instance, by the second deprotonation process that occurs in the presence of water. Similarly to the FD case, we observe an almost rigid shift of the molecular states (e.g., H_m) toward the conduction band of the substrate.

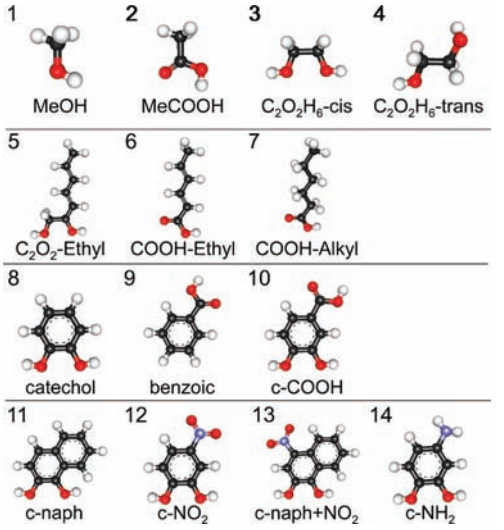

Figure 4. Atomic structure of the selected molecules described in the text.

In summary, a rationale can be drawn. As for many benzophenolic compounds, catechol is a weak acid (pK_a 8−10)[40] and may easily undergo oxygen deprotonation in order to increase the electronic conjugation of the attached phenyl ring. The presence of the dimerized ZnO($10\bar{1}0$) surface, which exposes more negatively charged oxygen atoms (i.e., behaving as a base), favors this process, leading spontaneously to the half-protonated geometry of Figure 2a. In vacuum, a second deprotonation is energetically unfavored since it would formally lead to a −2 charge state for the molecule (high electron concentration), without any further compensating change in the bonding path with the surface. On the other side, the pK_a value of hydroxyl groups is strongly dependent on the presence of water molecules that may change the chemical environment perceived by catechol. Indeed, passivation of surface dimers along with formation of more H bonds stabilize the negative charge on the molecular oxygens, lowering the pK_a value. This justifies the spontaneous double deprotonation observed in the *Wat* configuration but not in vacuum.

Our results show that the presence of molecular states in the gap (albeit at different energies) is not related to the number of deprotonated H^+ ions, but it is rather to be ascribed to the specific surface charge distribution and polarization field of the wurtzite ZnO surface.[41] This may not be the case for different surfaces, even for metal−oxides, such as tetragonal TiO_2 that has a completely different chemical environment and adsorption geometries.[12] These issues modify the molecule−substrate interaction as well as the electron distribution of the molecular oxygens and thus the band alignment with respect to the metal−oxide energy gap.

Gap-State Alignment. On the basis of the characterization of the optoelectronic properties of the catechol/ZnO interface, two questions arise: (i) what pins the molecular HOMO inside the ZnO gap, thus giving the staggered interface, and (ii) how can we modify the energy position of the molecular orbitals, in order to modulate the band alignment of the interface?

From the analysis of the electronic properties (see Figure 2b) we note that after adsorption the H_m state is still a purely molecular

state, not affected by the interaction with the surface. Thus, its energy position with respect to the surface gap should be dictated by its low ionization potential (I_p). To investigate the effect of the molecular ionization potential on the final band alignment of the interface, we considered a set of molecules (Figure 4) with different anchor and lateral attached groups and analyzed the different HOMO−LUMO alignment with respect to the band gap of the ZnO surface. Simulations are done in gas phase, and the energy levels are aligned to the vacuum level; the results are summarized in Figure 5. Atomic structures, total energies, and frontier HOMO−LUMO orbitals of the fully relaxed molecules are reported in the Supporting Information (section S4).

Catechol has one aromatic ring and two consecutive OH terminations that link to the surface. Both components contribute to the HOMO state laying in the ZnO gap. We decouple the effects of the two subsystems by considering the anchor group first. We analyzed three fully saturated attaching groups: namely, a single OH as in methanol MeOH (**1**) and a COOH group as in acetic acid MeCOOH (**2**) and the double OH termination $C_2O_2H_6$-*cis* (**3**) as in catechol. Methanol and acetic acid have a large gap and do not introduce states in the ZnO gap, as the HOMO energy is below the value of the valence band top of the surface (i.e., leading to formation of type I interfaces). On the contrary, the $C_2O_2H_6$-*cis* fragment sets the HOMO level deep inside the ZnO gap (type II interface), as in the case of catechol itself. We attribute this different behavior to the electrostatic repulsion between molecular oxygen atoms: methanol has a single oxygen lone pair, acetic acid has a lone pair and a double bond with the carbon atom, and $C_2O_2H_6$-*cis* has two close lone pairs that tend to repulse each other, destabilizing the system and reducing the ionization potential of the fragment, i.e., shifting the HOMO to higher energies. We proove this statement considering the $C_2O_2H_6$-*trans* group (**4**), where the oxygens are inverted with respect to the C−C bond. This structural modification reduces the O−O repulsion, giving a net lowering of the HOMO state energy, now very close to the VBT.

This interpretation is in perfect agreement also with the molecular peak displacements described above in the case of fully protonated and fully deprotonated configurations (Figure 3). Indeed, the FD systems (with and without water), which maximize the electrostatic repulsion in the anchor group, have molecular states (e.g., HOMO) very close to the ZnO CBM, while the opposite occurs for the FP case, where the presence of the attached protons screens the oxygen−oxygen repulsion.

In order to include the effect of electron delocalization, we consider a five-ethyl-long oligomer attached to both the C_2O_2 and the COOH terminations, labeled C_2O_2-Ethyl (**5**) and COOH-Ethyl (**6**), respectively. In both cases inclusion of a conjugated fragment shifts the HOMO states at higher energies with respect to the corresponding anchor groups. Saturation of the double C−C bonds in an alkyl chain (COOH-Alkyl, **7**) takes back the HOMO energy toward the ZnO VBT. In a similar way, we compare catechol (**8**) and benzoic acid (**9**), which have the same phenyl ring but different linking groups. As found previously, the COOH termination tends to increase the ionization potential, lowering the HOMO energy. However, the charge delocalization due to the aromatic ring influences the systems in the opposite direction. The coexistence of C_2O_2 and COOH groups (*c*-COOH, **10**) gives an intermediate result. Notably, following this trend, benzoic acid, whose sensitization properties have been long debated,[12,14,15] should form a type II interface with the ZnO surface. We conclude that the presence of

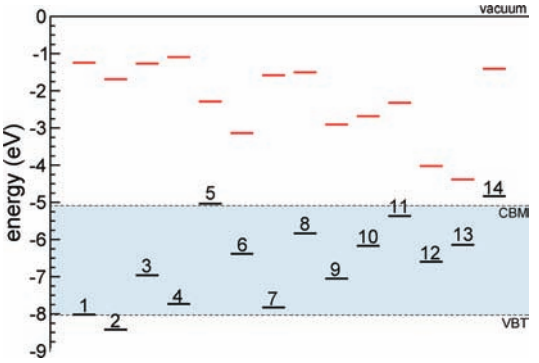

Figure 5. HOMO (black) and LUMO (red) energy alignment for the considered molecules in the gas phase, with respect to the vacuum level. Shaded area identifies the band gap of clean ZnO($10\bar{1}0$) surface. Labels refer to Figure 4.

molecular states in the ZnO gap is the result of the interplay between the oxygen repulsion of the anchor group and the presence of conjugated fragments. In particular, we suggest that the presence of C_2O_2 anchor terminations is sufficient to insert new states in the ZnO surface gap. Furthermore, the effects of charge delocalization seem to sum up linearly to those of the anchor groups, maintaining the ionization potential order imposed by pristine anchor groups I_p(COOH) < I_p(OH) < I_p(C_2O_2).

We finally take the catechol as the reference structure (prefix *c* in Figure 4) and show how to change the band alignment inside the gap by means of its chemical functionalization, in a similar spirit of ref 42 for tailoring the transport properties of single-molecule devices. Inclusion of a second ring in 1,2-dihydroxynaphthalene, labeled *c*-naph (**11**), increases the electron delocalization and reduces the ionization potential of the molecule. As a result, the HOMO level shifts upward and the HOMO−LUMO gap is reduced. This can be useful to increase the coupling between the molecule and the conduction band minimum of the substrate, but it reduces the voltage ($\Delta V = CBM - H_m$) that can be extracted from the interface. This behavior is in agreement with the observed red shifts in the UV−vis absorption spectra of catecholates adsorbed on TiO_2 nanoparticles as a function of the number of attached phenyl groups.[4]

Inclusion of the NO_2 unit (**12**), which is a strong electron acceptor, operates instead in the opposite direction: NO_2 polarizes the molecule, reducing the electron accumulation in the OH anchor group and thus the lone pair repulsion described above. Intermediate configurations may be achieved composing these two effects (aromaticity and electron localization) as shown in the case of *c*-naph + NO_2 (**13**), whose HOMO state is midway with respect to the *c*-naph and *c*-NO_2 case. An alternative to displace the HOMO state toward the conduction band, without reducing the gap, is given by inclusion of an electron donor group such as NH_2. The *c*-NH_2 molecule (**14**), having the HOMO orbitals beyond the CBM of the ZnO, acts as effective n-dopant for the system. We conclude that the aromaticity/electron conjugation and the electron acceptor capability of functional groups operate in opposite directions, shifting upward and downward, respectively, the molecular states within the ZnO gap.

To corroborate the interpretation implied by Figure 5, where the results in terms of energy levels of the isolated molecule are used to estimate the band offset at the interface between the molecule and the ZnO substrate, we also evaluated the electronic

dx.doi.org/10.1021/ja1101008 |*J. Am. Chem. Soc.* 2011, 133, 5893–5899

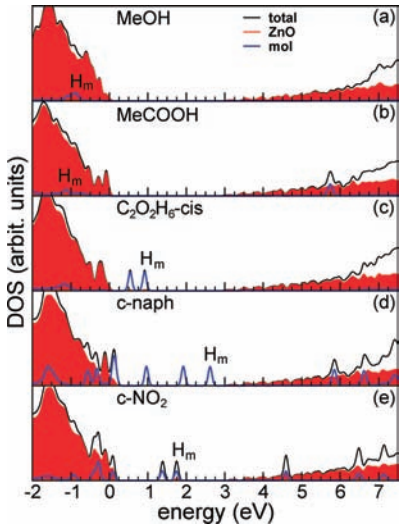

Figure 6. Total DOS (black line) and projected contributions on ZnO (shaded area) and molecule (blue line) for the different molecules chemisorbed on the ZnO substrate.

structure for a number of hybrid interfaces, whose atomic structures were obtained through a full geometry optimization. Figure 6 shows the total and projected DOS for selected chemisorbed molecules, taken as representative cases for different anchoring groups (hydroxyl, carboxylic, and dihydroxyl groups in panels a, b, and c), as well as for different chemical functionalization of the benzene ring (through a further aromatic ring and a NO_2 group in panels d and e). A direct comparison between the electronic structures of the real interfaces (Figure 6) and the band alignments expected starting from the single-molecule results (Figure 5, molecules **1**−**3**, **11**, and **12**) validates the latter predictions, at least qualitatively. In fact, the trends on the HOMO position within the ZnO gap are always reproduced; the only difference is given by the absolute value of the HOMO energy that turns out to be systematically overestimated by the single-molecule-based estimates. This can be traced back to the charge redistribution occurring at the real interface due to the Zn−O bond formation, associated to an interface polarization effect.

At this point, a paradigm for the best-suited surface functionalization can be definitely drawn: in the case of applications that require reasonably high ΔV voltages (e.g., as solar cells) or p-like behavior, inclusion of electron acceptor functional groups is preferred. On the contrary, in order to have n-like materials (e.g., transparent conducting oxides) or for devices working in the infrared regime, inclusion of aromatic systems is preferred. A proper combination of the two allows for intermediate configurations.

CONCLUSIONS

In this paper we studied the structural and optoelectronic properties of a prototypical catechol/ZnO($10\bar{1}0$) surface by means of ab initio DFT calculations. The catechol adsorbs on the surface, forming two Zn−O chemical bonds through the hydroxyl terminations of the molecule. The electronic structure of the hybrid system is consistent with a type II interface, characterized by the presence of molecular states in the gap that efficiently reduce the optical gap and allow for an ultrafast dye-to-substrate electron injection. We demonstrate that the origin of this staggered band alignment is due to the specific lone-pair interaction between the oxygen atoms along with the aromatic nature of the phenyl ring. Finally, we provide a simple and predictive paradigm to selectively tune the band alignment at the ZnO interface and obtain the best-suited properties for selected optoelectronic applications, without performing explicitly the complete interface simulation.

ASSOCIATED CONTENT

Supporting Information. Convergence accuracy tests on slab thickness (section S1) and DFT+U correction (section S2), details on electronic structure analysis (section S3), and total energies and atomic coordinates of optimized molecular structures (section S4). This material is available free of charge via the Internet at http://pubs.acs.org.

AUTHOR INFORMATION

Corresponding Author

arrigo.calzolari@unimore.it

Present Addresses

[⊥]Centro S3, CNR-Istituto di Nanoscienze, I-41125 Modena, Italy.

ACKNOWLEDGMENT

We thank Sylvie Rangan for fruitful discussions. This work was partially funded by Regione Emilia-Romagna through project "Prominer" and by CariTRO through the project "DAFNE". Computational resources were provided at CINECA by CNR-DMD.

REFERENCES

(1) Kamat, P.; Huehn, R.; Nicolaescu, R. *J. Phys. Chem. B* **2002**, *106*, 788–794.
(2) Maeda, K.; Takata, T.; Hara, M.; Saito, N.; Inoue, Y.; K. Domen, H. K. *J. Am. Chem. Soc.* **2005**, *127*, 8286–8287.
(3) Galoppini, E. *Coord. Chem. Rev.* **2004**, *248*, 1283–1297.
(4) Janković, I. A.; Šaponjić, Z. V.; Čomor, M. I.; Nedeljković, J. M. *J. Phys. Chem. C* **2009**, *113*, 12645–12652.
(5) Macyk, W.; Szaciłowski, K.; Stochel, G.; Marta BuchalskC, P. Ł.; Joanna, K. *Coord. Chem. Rev.* **2010**, *254*, 2687–2701.
(6) O'Regan, B.; Grätzel, M. *Nature (London)* **1991**, *353*, 737–740.
(7) Quintana, M.; Edvinsson, T.; Hagfeldt, A.; Boschloo, G. *J. Phys. Chem. C* **2007**, *111*, 1035–1041.
(8) Klimov, V. I.; Ivanov, S. A.; Nanda, J.; Achermann, M.; Bezel, I.; McGuire, J. A.; Piryatinski, A. *Nature (London)* **2008**, *447*, 441–446.
(9) Ramakrishna, G.; Ghosh, H. N. *Langmuir* **2003**, *19*, 3006–3012.
(10) Rangan, S.; Theisen, J.-P.; Bersch, E.; Bartynski, R. *Appl. Surf. Sci.* **2010**, *256*, 4829–4833.
(11) Gundlach, L.; Ernstorfer, R.; Willig, F. *Phys. Rev. B* **2006**, *74*, 035324 (1−10).
(12) Li, S.-H.; Wang, J. G.; Jacobson, P.; Gong, X.-Q.; Selloni, A.; Diebold, U. *J. Am. Chem. Soc.* **2009**, *131*, 980–984.
(13) Redfern, P.; Zapol, P.; Curtis, L.; Rajh, T.; Thurnauer, M. *J. Phys. Chem. B* **2003**, *107*, 11419–11427.
(14) Rego, L. G.; Batista, V. S. *J. Am. Chem. Soc.* **2003**, *125*, 7989–7997.
(15) Duncan, W.; Prezhdo, O. V. *J. Phys. Chem. B* **2005**, *109*, 365–373.
(16) Meyer, B.; Marx, D.; Dulub, O.; Diebold, U.; Kunat, M.; Langenberg, D.; Woll, C. *Angew. Chem., Int. Ed.* **2004**, *43*, 6641–6645.

(17) Savio, L.; Celasco, E.; Vattuone, L.; Rocca, M. *J. Phys. Chem. B* **20046**, *108*, 7771–7778.
(18) Gong, X.-Q.; Selloni, A.; Vittadini, A. *J. Phys. Chem. B* **2006**, *110*, 2804–2811.
(19) Calzolari, A.; Catellani, A. *J. Phys. Chem. C* **2009**, *113*, 2896–2902.
(20) Tao, F.; Bernasek, S. L.; Xu, G.-Q. *Chem. Rev.* **2009**, *109*, 3991–4024.
(21) Alivisatos, A. P. *Nat. Biotechnol.* **2004**, *22*, 47–52.
(22) Tessler, N.; Medvedev, V.; Kazes, M.; Kan, S.; Banin, U. *Science* **2002**, *295*, 1506–1508.
(23) Coe, S.; Woo, W.-K.; Bawendi, M.; Bulović, V. *Nature (London)* **2002**, *420*, 800–803.
(24) Gur, I.; Fromer, N.; Geier, M. L.; Alivisatos, A. P. *Science* **2005**, *310*, 462–465.
(25) Schrier, J.; Demchenko, D. O.; Wang, L.-W. *Nano Lett.* **2007**, *7*, 2377–2382.
(26) Gross, D.; susha, A. S.; Klar, T. A.; Da Como, E.; Rogach, A. L.; Feldmann, J. *Nano Lett.* **2008**, *8*, 14862–1485.
(27) Hewa-Kasakarage, N. N.; El-Khoury, P. Z.; Tarnovsky, A. N.; Kirsanova, M.; Nemitz, I.; Nemchinov, A.; Zamkov, M. *ACS Nano* **2010**, *4*, 1837–1844.
(28) Calzolari, A.; Ruini, A.; Cavazzoni, C.; Caldas, M. J. *J. Phys. Chem. C* **2010**, *114*, 19535–19539.
(29) Giannozzi, P.; Baroni, S.; Bonini, N.; Calandra, M.; Car, R.; Cavazzoni, C.; Ceresoli, D.; Chiarotti, G. L.; Cococcioni, M.; Dabo, I.; Dal Corso, A.; de Gironcoli, S.; Fabris, S.; Fratesi, G.; Gebauer, R.; Gerstmann, U.; Gougoussis, C.; Kokalj, A.; Lazzeri, M.; Martin-Samos, L.; Marzari, N.; Mauri, F.; Mazzarello, R.; Paolini, S.; Pasquarello, A.; Paulatto, L.; Sbraccia, C.; Scandolo, S.; Sclauzero, G.; Seitsonen, A. P.; Smogunov, A.; Umari, P.; Wentzcovitch, R. M. *J. Phys.: Condens. Matter* **2009**, *21*, 395502.See also www.quantum-espresso.org.
(30) Perdew, J. P.; Burke, K.; Ernzerhof, M. *Phys. Rev. Lett.* **1996**, *77*, 3865–3868.
(31) Vanderbilt, D. *Phys. Rev. B* **1990**, *41*, R7892–R7895.
(32) Schleife, A.; Fuchs, F.; Furthmüller, J.; Bechstedt, F. *Phys. Rev. B* **2006**, *73*, 245212 (1−14).
(33) Shih, B.-C.; Xue, Y.; Zhang, P.; Cohen, M. L.; Louie, S. G. *Phys. Rev. Lett.* **2010**, *105*, 146401 (1−4).
(34) Janotti, A.; Segev, D.; Van de Walle, C. G. *Phys. Rev. B* **2006**, *74*, 045202 (1−9).
(35) Dong, Y.; Brillson, L. *J. Electron. Mater.* **2008**, *37*, 743–748.
(36) Vogel, D.; Krüger, P.; Pollmann, J. *Phys. Rev. B* **1996**, *54*, 5495–5511.
(37) Cherepy, N. J.; Smestad, G. P.; Grätzel, M.; Zhang, J. Z. *J. Phys. Chem. B* **1997**, *101*, 9342–9351.
(38) Calzolari, A.; Varsano, D.; Ruini, A.; Catellani, A.; Tel-Vered, R.; Yildiz, H. B.; Ovits, O.; Willner, I. *J. Phys. Chem. A* **2009**, *113*, 8801–8810.
(39) Calzolari, A.; Monti, S.; Ruini, A.; Catellani, A. *J. Chem. Phys.* **2010**, *132*, 114304 (1−9).
(40) Bouchoux, G.; Defaye, D.; McMahon, T.; Likholyot, A.; Mó, O.; Yánez, M. *Chem.—Eur. J.* **2002**, *8*, 2900–2909.
(41) Cicero, G.; Ferretti, A.; Catellani, A. *Phys. Rev. B* **2009**, *80*, 201304.
(42) Venkataraman, L.; Park, Y. S.; Whalley, A. C.; Nuckolls, C.; Hybertsen, M. S.; Steigerwald, M. L. *Nano Lett.* **2007**, *7*, 502.